# Supporting Information for:

# Photophysical Processes in Rhenium(I) Diiminetricarbonyl Arylisocyanides Featuring Three Interacting Triplet Excited States

*Joseph M Favale Jr., Evgeny O. Danilov, James E. Yarnell, and Felix N. Castellano**

Department of Chemistry, North Carolina State University (NCSU), Raleigh, NC, 27695-8204, United States

EMAIL ADDRESS: fncastel@ncsu.edu

* To whom correspondence should be addressed. Phone: (419) 372-7513 Fax: (419) 372-9809

## Detailed Synthetic Procedures

### General Experimental Considerations

All reagents and solvents used in the synthetic procedures were obtained from commercial sources and used as received, unless otherwise noted. Free organic isocyanides possess a particularly disagreeable odor, in particular ligand 7a. Due to this, all reactions to form the isocyanide group and any handling of isocyanides should be performed in a well-ventilated fume hood.

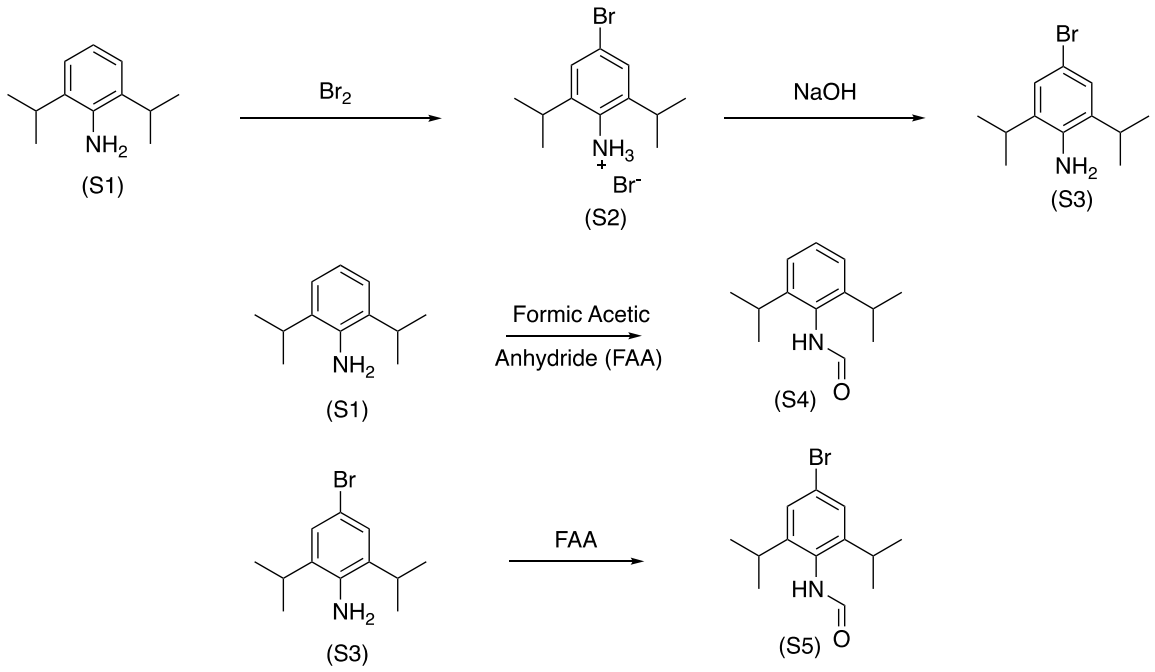


**Figure S1:** General synthetic pathway of aniline functionalization and protection.

### Synthesis of 4-Bromo-2,6-diisopropylaniline (S3)

Prepared based on previously published procedure.[1] 2,6-diisopropylaniline (**S1**) (20 mL, 0.106 mol) was dissolved in dichloromethane/methanol (1:1 v/v, 100 mL). To this stirring solution, a solution of $Br_2$ (5.5 mL, 0.108 mol) was added dropwise via addition funnel. The reaction was stirred at room temperature for 12 h and the solvent was evaporated. The solid product was dissolved in a minimal amount of dichloromethane and recrystallized by layered addition of hexanes, yielding pure 4-bromo-2,6-diisopropylaniline hydrobromide (**S2**) as a white crystalline solid, which was used as obtained.

This solid was added to a solution of 20% aqueous NaOH (50 mL) and stirred for 2 h. This solution was extracted with diethyl ether (3 x 50 mL) and the combined extracts were washed twice with saturated sodium bicarbonate solution and dried with sodium sulfate. Filtration and evaporation of the solvent yielded the product as a pure oil. Yield: 19.65 g, 72%. $^1$H NMR (400 MHz, $CDCl_3$): δ 7.19 (d, 2H, $J$ = 6.8 Hz), 3.71 (br s, 2H), 2.91 (sep, 2H, $J$ = 6.8 Hz), 1.30 (d, 12H, $J$ = 6.8 Hz).

**Synthesis of N-formyl-2,6-diisopropylaniline (S4)**

Prepared based on previously published procedure.[2] In a 500 mL round bottomed flask, acetic anhydride (40 mL) was cooled to 0 ℃ and formic acid (20 mL) was added dropwise via syringe. This solution was warmed with stirring to 50 ℃ for 2 h then cooled back to 0 ℃. 2,6-diisopropylaniline (**S1**) (5 g, 28.20 mmol) was added via syringe and the reaction was allowed to warm to room temperature. After stirring for 1 h, the reaction was cooled to 0 ℃ and 300 mL of 0 ℃ DI water was added, yielding a light pink suspension. The solid product was vacuum filtered and washed with 1 L of DI water. The solid was dried under vacuum overnight to yield pure product as an off-white solid. Yield: 5.46 g, 94%. $^1$H NMR (400 MHz, $CD_2Cl_2$): Mixture of isomers. δ 8.47 and 8.01 (m, 1H), 7.36-7.29 (m, 1H), 7.21 (m, 1H), 7.19 and 6.81 (m, 1H), 3.27-3.06 (m, 2H) 1.20 (m, 12H).

**Synthesis of N-formyl-4-bromo-2,6-diisopropylaniline (S5)**

Prepared based on previously published procedure.[2] In a 500 mL round bottomed flask, acetic anhydride (40 mL) was cooled to 0 ℃ and formic acid (20 mL) was added dropwise via syringe. This solution was warmed with stirring to 50 ℃ for 2 h then cooled back to 0 ℃. 4-bromo-2,6-diisopropylaniline (**S3**) (5 g, 19.517 mmol) was added via syringe and the reaction was allowed to warm to room temperature. After stirring for 1 h, the reaction was cooled to 0 ℃ and 300 mL of 0 ℃ DI water was added, yielding a light pink suspension. The solid product was vacuum filtered and washed with 1 L of DI water. The solid was dried under vacuum overnight to yield pure product as an off-white solid. Yield: 5.32 g, 96%. $^1$H NMR (400 MHz, $CD_2Cl_2$): Mixture of isomers. δ 8.39 and 7.96 (m, 1H), 7.32 and 7.30 (m, 2H), 7.04 and 6.82 (br s, 1H), 3.17 and 3.05 (m, 2H), 1.17 (m, 12H).

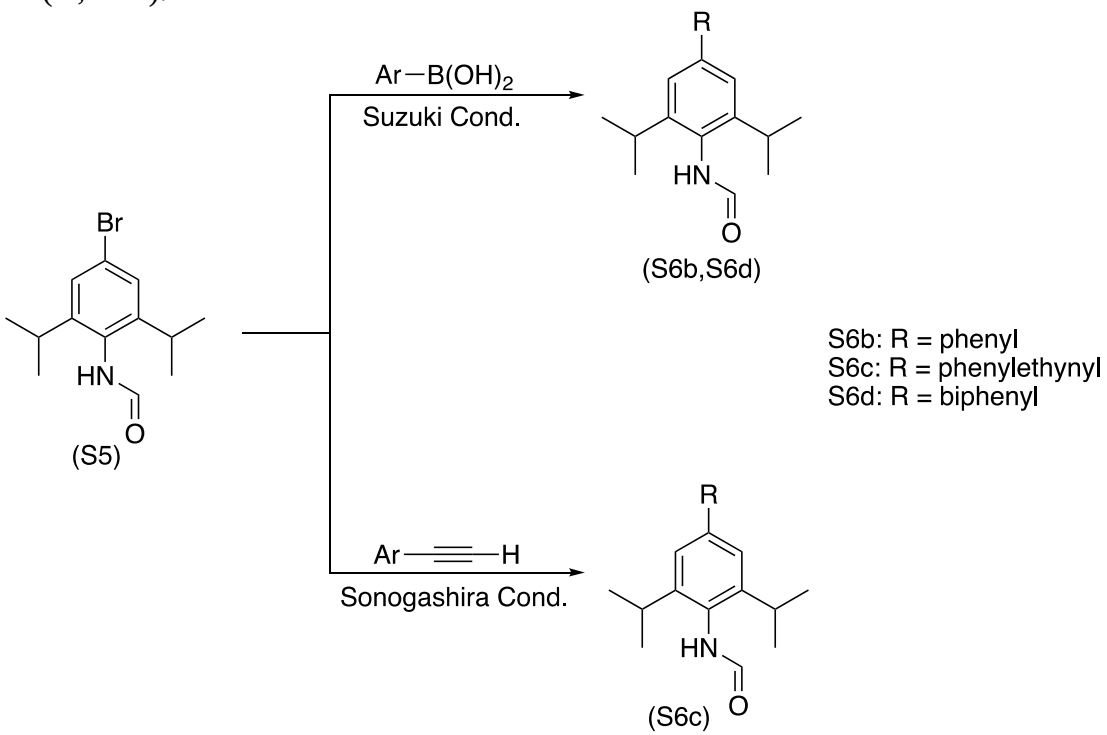


**Figure S2:** General synthetic pathway of coupling reactions.

**Synthesis of N-formyl-4-phenyl-2,6-diisopropylaniline (S6b)**
In a 100 mL two-necked round bottomed flask, fitted with a reflux condenser, N-formyl-4-bromo-2,6-diisopropylaniline (**S5**) (750 mg, 2.64 mmol), phenylboronic acid (355 mg, 2.91 mmol), palladium(II) acetate (40 mg), triphenylphosphine (80 mg), and cesium carbonate (2.5 g) were degassed via vacuum and nitrogen backfill cycles at least 3 times and placed under positive pressure $N_2$. To the solids, a bubble degassed solvent mixture of 80 mL tetrahydrofuran and 5 mL DI water was added and brought to reflux at 75 °C for 24 h. After cooling to room temperature, the reaction solution was passed through a celite plug washed with a small amount of dichloromethane and the filtrate was washed with saturated sodium bicarbonate solution. The organic layer dried and evaporated yielding an off-white solid, which was recrystallized from dichloromethane and pentane. Yield: 520 mg, 70% $^1$H NMR (400 MHz, $CD_2Cl_2$): Mixture of isomers. δ 8.47 and 8.06 (m, 1H), 7.60 (m, 2H), 7.48-7.32 (m, 5H), 6.89 and 6.83 (m, 1H), 3.28 and 3.16 (m, 2H), 1.26 (m, 12H).

**Synthesis of N-formyl-4-phenylethynyl-2,6-diisopropylaniline (S6c)**
In a 50 mL two-necked round bottomed flask, N-formyl-4-bromo-2,6-diisopropylaniline (**S5)** (500 mg, 1.76 mmol), $Pd(PPh_3)_2Cl_2$ (25 mg), triphenylphosphine (10 mg) and copper (I) iodide (3 mg) were deoxygenated via vacuum and nitrogen backfill cycles at least 3 times and placed under positive pressure $N_2$. To this flask, bubble degassed triethylamine (20 mL) was added via syringe and all solids allowed to dissolve. Phenylacetylene (0.2 mL, 1.82 mmol) was added via syringe and the reaction heated to 65 °C for 12 h. After cooling to room temperature, the reaction mixture was poured over a silica plug and eluted with diethyl ether. Evaporation of solvent and drying under vacuum overnight yielded product as an off-white to yellowish solid. Yield: 378 mg, 74%. $^1$H NMR (400 MHz, $CD_2Cl_2$): Mixture of isomers. δ 8.45 and 8.00 (m, 1H), 7.56 (m, 2H), 7.38 (m, 5H), 6.86 and 6.78 (m, 1H), 3.22 and 3.09 (m, 2H), 1.23 (m, 12H).

**Synthesis of N-formyl-4-biphenyl-2,6-diisopropylaniline (S6d)**
In a 100 mL two-necked round bottomed flask, fitted with a reflux condenser, N-formyl-4-bromo-2,6-diisopropylaniline (**S5**) (775 mg, 2.73 mmol), 4-biphenylboronic acid (560 mg, 2.83 mmol), palladium(II) acetate (40 mg), triphenylphosphine (80 mg), and cesium carbonate (2.5 g) were degassed via vacuum and nitrogen backfill cycles at least 3 times and placed under positive pressure $N_2$. To the solids, a bubble degassed solvent mixture of 80 mL tetrahydrofuran and 5 mL DI water was added and brought to reflux at 75 °C for 24 h. After cooling to room temperature, the reaction solution was passed through a celite plug washed with a small amount of dichloromethane and the filtrate was washed with saturated sodium bicarbonate solution. The organic layer dried and evaporated yielding an off-white solid, which was recrystallized from dichloromethane and pentane. Yield: 685 mg, 70% $^1$H NMR (400 MHz, $CD_2Cl_2$): Mixture of isomers. δ 8.45 and 8.07 (m, 1H), 7.71-7.65 (m, 6H), 7.50-7.45 (m, 4H), 7.40-7.35 (m, 1H), 6.96 and 6.87 (m, 1H), 3.29 and 3.18 (m, 2H), 1.28 (m, 12H).

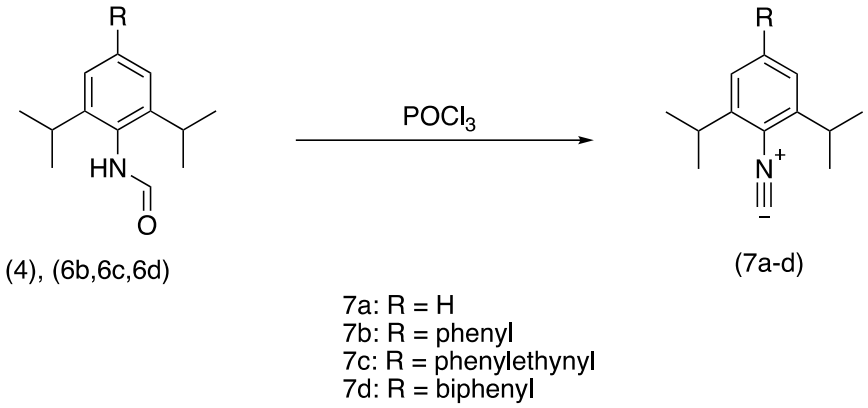


**Figure S3:** General synthetic pathway of free isocyanide formation.

**Synthesis of 2,6-Diisopropylphenylisocyanide (S7a)**

Prepared based on previously published procedure.[2] In a 250 mL round bottomed flask, N-formyl-2,6-diisopropylaniline (**S4**) (1g, 4.87 mmol) was dissolved in 50 mL of dichloromethane and cooled to 0 °C. Diisopropylamine (2.5 mL) was added via syringe followed by $POCl_3$ (0.6 mL), added dropwise over 20 min. The reaction was allowed to warm to room temperature and stirred for 2 h. A concentrated solution of $Na_2CO_3$ was added to the reaction mixture and the biphasic mixture was rigorously stirred overnight. The organic layer was separated, washed with sodium bicarbonate solution and evaporated. The desired product was purified on a silica column eluted with dichloromethane. Yield: 474 mg, 52%. $^1$H NMR (400 MHz, $CDCl_3$): δ 7.33 (t, 1H, *J* = 7.8 Hz), 7.18 (d, 2H, *J* = 7.8 Hz), 3.38 (sep, 2H, *J* = 6.9 Hz), 1.27 (d, 12H, *J* = 6.9 Hz). FTIR (ATR, $cm^{-1}$): $\upsilon_{CN}$ = 2113 (s)

**Synthesis of 4-Phenyl-2,6-diisopropylphenylisocyanide (S7b)**

In a 250 mL round bottomed flask, N-formyl-4-phenyl-2,6-diisopropylaniline (**S6B**) (1g, 3.80 mmol) was dissolved in 50 mL of dichloromethane and cooled to 0 °C. Diisopropylamine (2.5 mL) was added via syringe followed by $POCl_3$ (0.6 mL), added dropwise over 20 min. The reaction was allowed to warm to room temperature and stirred for 2 h. A concentrated solution of $Na_2CO_3$ was added to the reaction mixture and the biphasic mixture was rigorously stirred overnight. The organic layer was separated, washed with sodium bicarbonate solution and evaporated. The desired product was purified on a silica column eluted with dichloromethane. Yield: 590 mg, 59%. $^1$H NMR (400 MHz, $CD_2Cl_2$): δ 7.60 (m, 2H), 7.47 (m, 2H), 7.41 (m, 3H), 3.43 (sep, 2H, *J* = 6.9 Hz), 1.33 (d, 12H, *J* = 6.9 Hz). FTIR (ATR, $cm^{-1}$): $\upsilon_{CN}$ = 2111 (s)

**Synthesis of 4-Phenylethynyl-2,6-diisopropylphenylisocyanide (S7c)**

In a 250 mL round bottomed flask, N-formyl-4-phenylethynyl-2,6-diisopropylaniline (**S6C**) (1g, 3.27 mmol) was dissolved in 50 mL of dichloromethane and cooled to 0 °C. Diisopropylamine (2.5 mL) was added via syringe followed by $POCl_3$ (0.6 mL) added dropwise over 20 min. The reaction was allowed to warm to room temperature and stirred for 2 h. A concentrated solution of $Na_2CO_3$ was added to the reaction mixture and the

biphasic mixture was rigorously stirred overnight. The organic layer was separated, washed with sodium bicarbonate solution and evaporated. The desired product was purified on a silica plug eluted with dichloromethane. Yield: 414 mg, 44%. $^1$H NMR (400 MHz, $CD_2Cl_2$): δ 7.54 (m, 2H), 7.36 (m, 5H), 3.36 (sep, 2H, *J* = 6.9 Hz), 1.28 (d, 12 H, *J* = 6.9 Hz). FTIR (ATR, cm$^{-1}$) $\upsilon_{CN}$ = 2115 (s), $\upsilon_{CC}$ = 2219 (w)

**Synthesis of 4-Biphenyl-2,6-diisopropylphenylisocyanide (S7d)**

In a 250 mL round bottomed flask, N-formyl-4-biphenyl-2,6-diisopropylaniline (**S7d**) (1g, 2.80 mmol) was dissolved in 50 mL of dichloromethane and cooled to 0 °C. Diisopropylamine (2.5 mL) was added via syringe followed by $POCl_3$ (0.6 mL), added dropwise over 20 min. The reaction was allowed to warm to room temperature and stirred for 2 h. A concentrated solution of $Na_2CO_3$ was added to the reaction mixture and the biphasic mixture was rigorously stirred overnight. The organic layer was separated, washed with sodium bicarbonate solution and evaporated. The desired product was purified on a silica column eluted with dichloromethane. Yield: 617 mg, 65%. $^1$H NMR (400 MHz, $CD_2Cl_2$): δ 7.74-7.66 (m, 6H), 7.48 (m, 2H), 7.45 (s, 2H), 7.38 (m, 1H), 3.45 (sep, 2H, *J* = 6.9 Hz), 1.34 (d, 12H, *J* = 6.9 Hz). FTIR (ATR, cm$^{-1}$): $\upsilon_{CN}$ = 2115 (s)

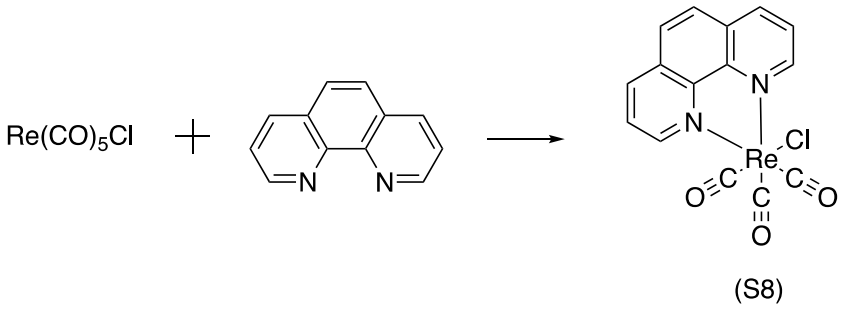


(S8)

**Figure S4:** General synthetic pathway of Re(phen)$(CO)_3$Cl starting material.

**Synthesis of Re(phen)$(CO)_3$Cl (S8)**

Synthesized based on previously published procedure.[3] To a 2-necked round bottomed flask with reflux condenser, solid rhenium(I) pentacarbonyl chloride (1.00 g, 2.76 mmol) and 1,10-phenanthroline (500 mg, 2.77 mmol) were degassed by at least two cycles of vacuum-$N_2$ backfill and placed under positive $N_2$ pressure. Freshly distilled toluene (75 mL) was added to these solids via syringe and the reaction was heated to reflux at 115 °C for 4 h. After this time, the reaction was cooled to 0 °C in a freezer to induce precipitation. The solids were filtered and washed with excess toluene and dried under vacuum to yield pure yellow solid product. Yield: 1.28 g, 95%. $^1$H NMR (400 MHz, $CD_2Cl_2$): δ 9.38 (dd, 2H, *J* = 5.1, 1.4 Hz), 8.61 (dd, 2H, *J* = 8.2, 1.4 Hz), 8.07 (s, 2H), 7.91 (dd, 2H, *J* = 8.2, 5.1 Hz). $\upsilon_{CO}$ = 2013 (s), 1886 (s)

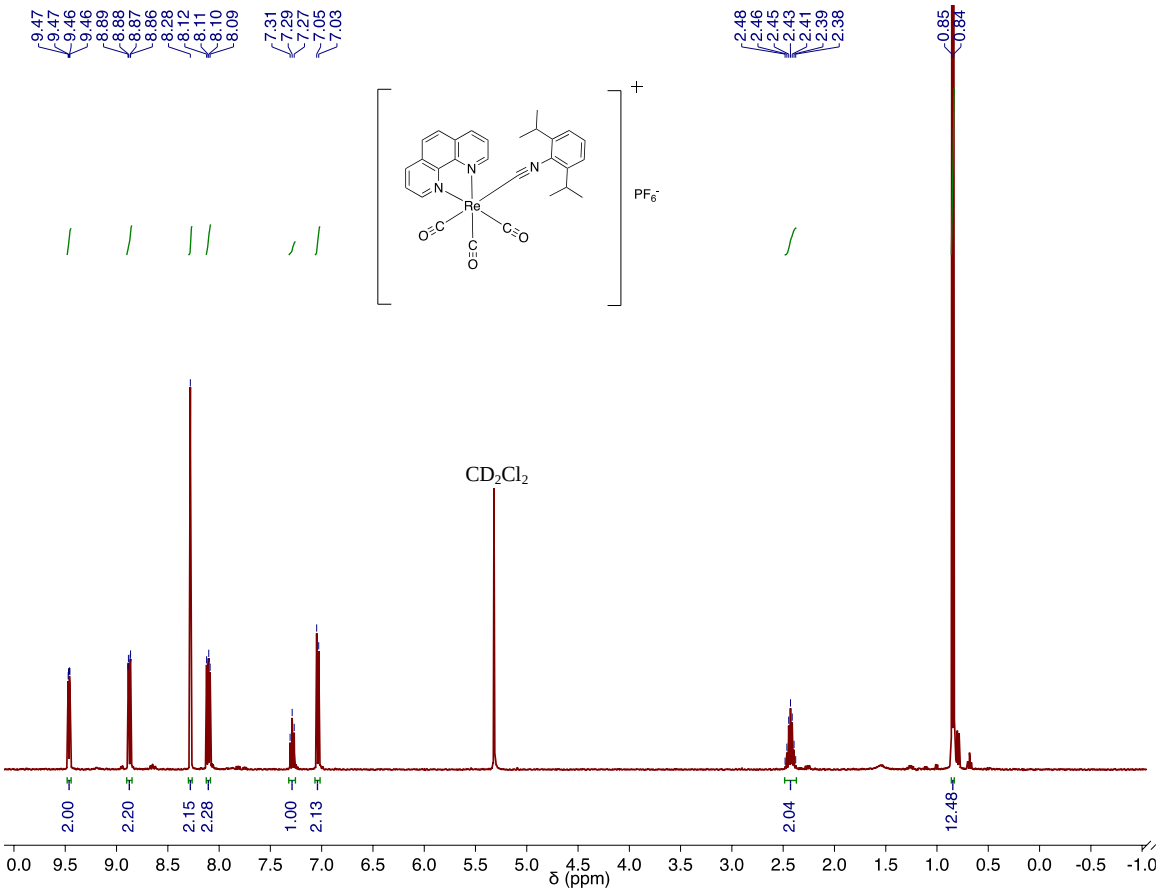


**Figure S5:** $^{1}$H NMR of **1** in $CD_2Cl_2$ (400 MHz)

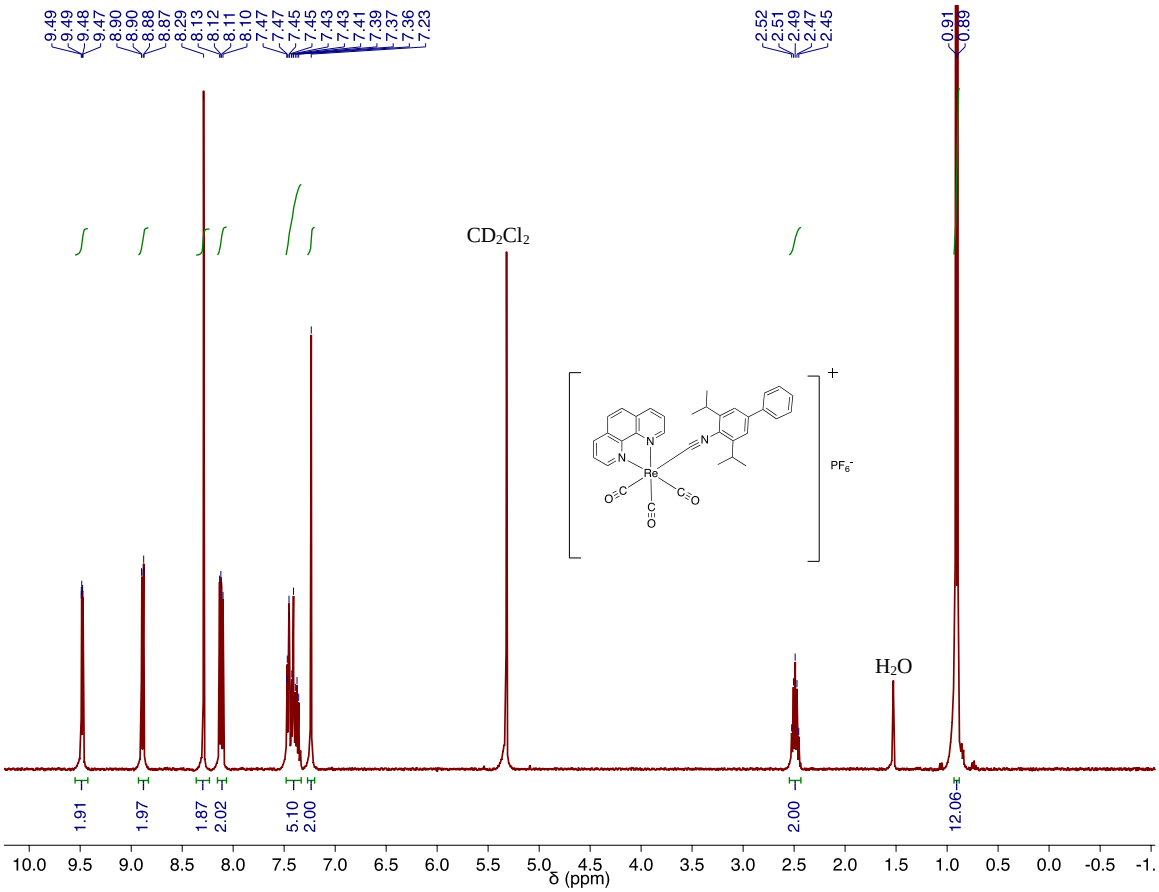


**Figure S6:** $^{1}$H NMR of **2** in $CD_2Cl_2$ (400 MHz)

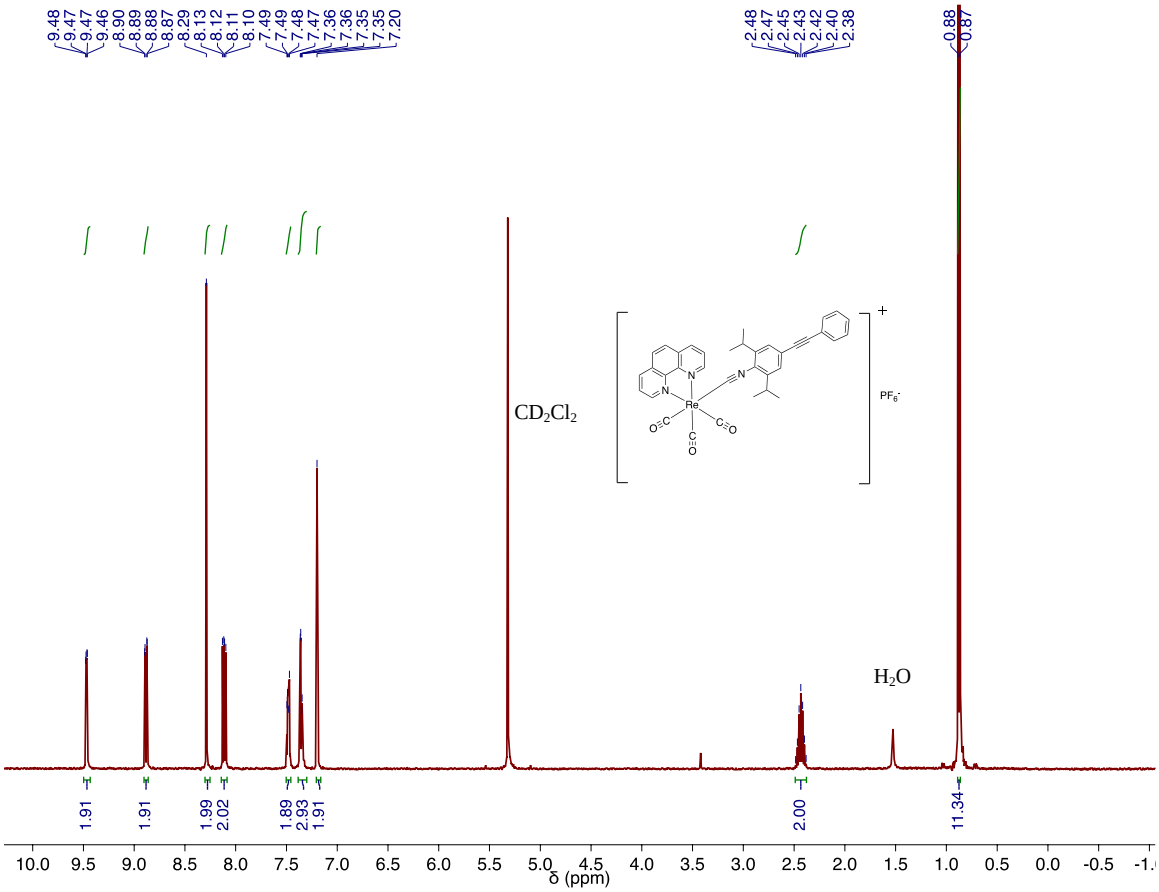


**Figure S7:** $^{1}$H NMR of **3** in $CD_2Cl_2$ (400 MHz)

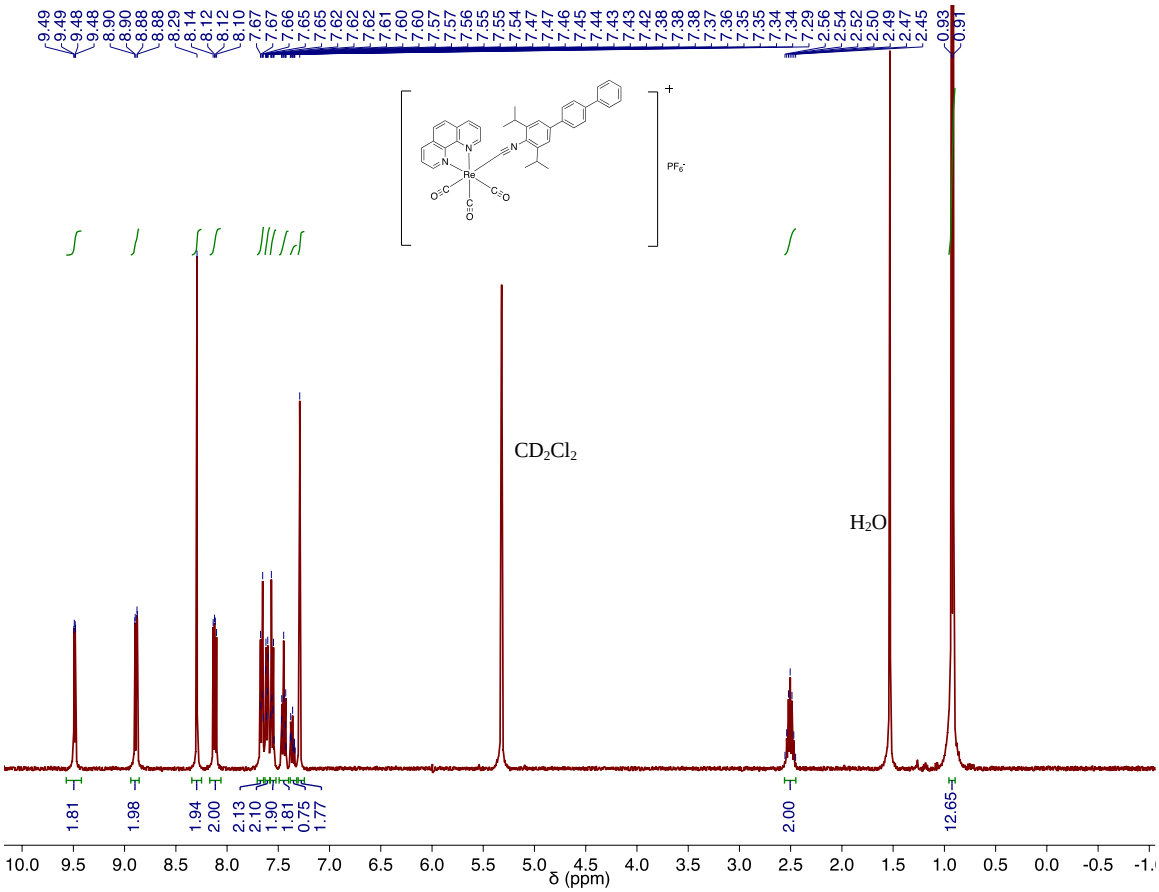


**Figure S8:** $^{1}$H NMR of **4** in $CD_2Cl_2$ (400 MHz)

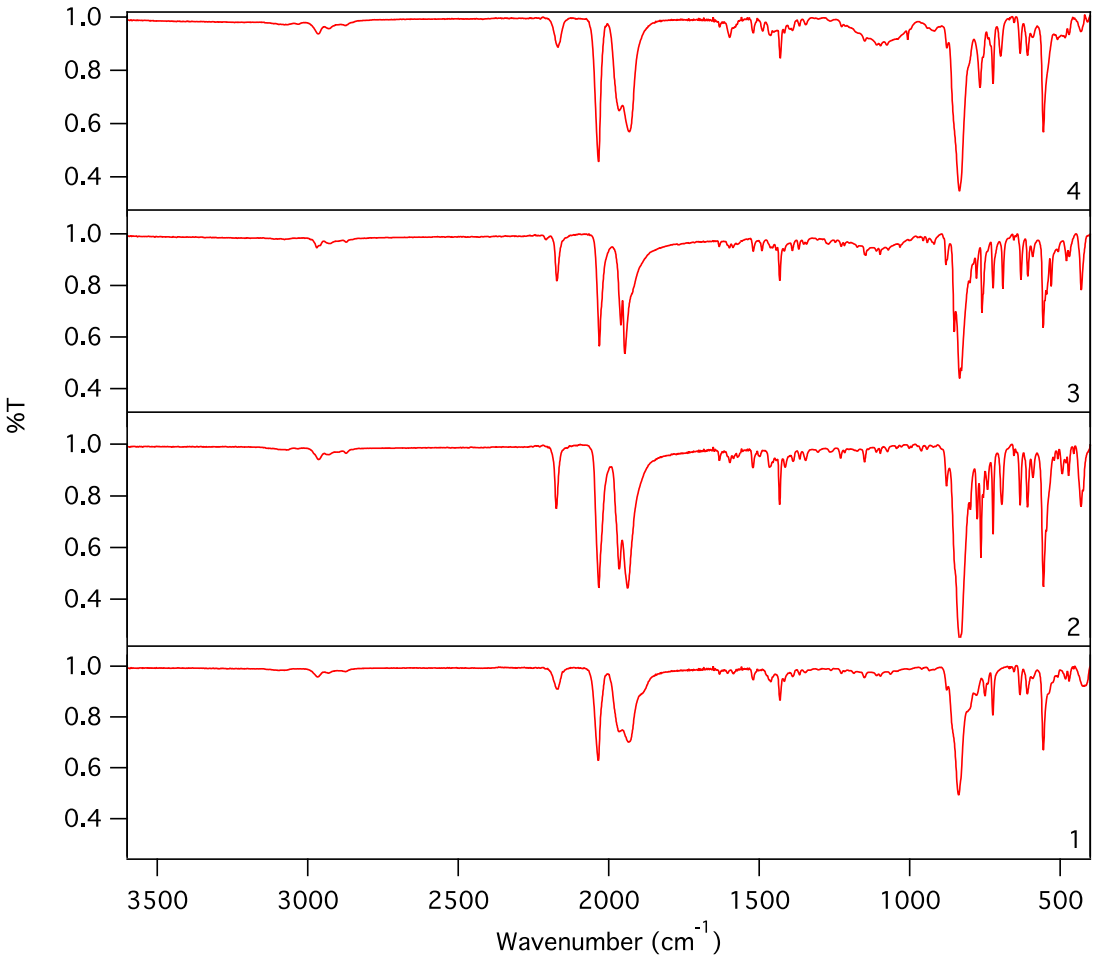


**Figure S9:** FTIR-ATR spectra of **1**-**4** solid samples.

**Table S1**. Calculated frontier orbital energies of the molecules in this study.[a]

| Molecular Orbital | **1** | **2** | **3** | **4** |
|---|---|---|---|---|
| LUMO+2 | -2.352 eV | -2.442 eV | -2.643 eV | -2.475 eV |
| LUMO+1 | -2.865 eV | -2.866 eV | -2.872 eV | -2.866 eV |
| LUMO | -3.080 eV | -3.082 eV | -3.089 eV | -3.082 eV |
| HOMO | -7.274 eV | -6.970 eV | -6.755 eV | -6.676 eV |
| HOMO-1 | -7.549 eV | -7.552 eV | -7.521 eV | -7.359 eV |
| HOMO-2 | -7.642 eV | -7.604 eV | -7.566 eV | -7.550 eV |

[a] Calculations performed at DFT//M06/Def2-SVP/SDD level of theory.

[Re(phen)(CO)$_3$(DippCN)](PF$_6$)

| Transitions | Energy/eV (nm) | *f* | Composition | CI |
|---|---|---|---|---|
| $S_0 \rightarrow S_1$ | 3.26 (381) | 0.0023 | H → L<br>H-4 → L | 0.69210<br>0.11035 |
| $S_0 \rightarrow S_2$ | 3.48 (357) | 0.0295 | H-2 → L<br>H-1 → L<br>H → L+1 | 0.36310<br>0.56396<br>0.18345 |
| $S_0 \rightarrow S_3$ | 3.53 (351) | 0.0185 | H-2 → L<br>H-1 → L<br>H → L+1 | 0.56354<br>0.24366<br>0.32860 |
| $S_0 \rightarrow S_4$ | 3.61 (343) | 0.0716 | H-2 → L<br>H-1 → L<br>H → L+1 | 0.20583<br>0.31332<br>0.58398 |

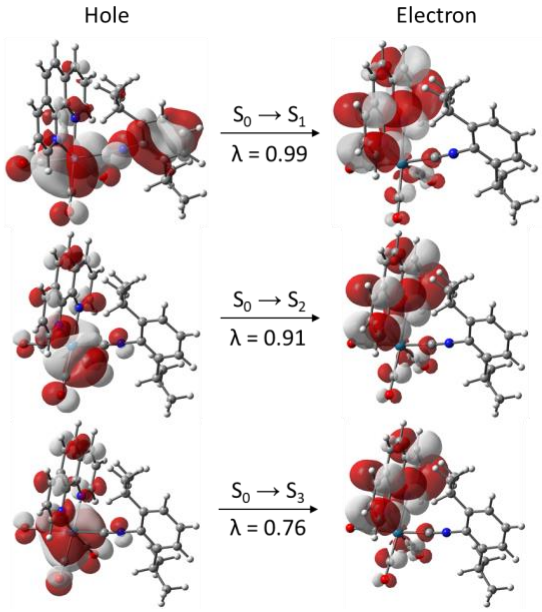


**Figure S10**. (Left) Energies and composition of the lowest energy singlet transitions in **1**. (Right) The natural transition orbitals of transitions $S_0 \rightarrow S_1$, $S_0 \rightarrow S_2$, and $S_0 \rightarrow S_3$ in **1**; λ is the fraction of the hole–particle contribution to the excitation. Calculations performed at DFT//M06/Def2-SVP/SDD level of theory.

[Re(phen)(CO)$_3$(PhDippCN)](PF$_6$)

| Transitions | Energy/eV (nm) | *f* | Composition | CI |
|---|---|---|---|---|
| $S_0 \rightarrow S_1$ | 3.15 (394) | 0.0035 | H-2 → L<br>H → L | 0.27252<br>0.64586 |
| $S_0 \rightarrow S_2$ | 3.43 (361) | 0.0028 | H-2 → L+1<br>H-1 → L<br>H → L+1 | 0.21447<br>0.28593<br>0.60200 |
| $S_0 \rightarrow S_4$ | 3.54 (350) | 0.1347 | H-3 → L<br>H-2 → L<br>H-1 → L<br>H → L+1<br>H → L+2 | 0.47005<br>0.17227<br>0.40209<br>0.17553<br>0.20939 |
| $S_0 \rightarrow S_5$ | 3.68 (337) | 0.6774 | H-2 → L+2<br>H-2 → L+5<br>H-1 → L<br>H-1 → L+3<br>H → L+2 | 0.15059<br>0.10401<br>0.23524<br>0.10757<br>0.59917 |

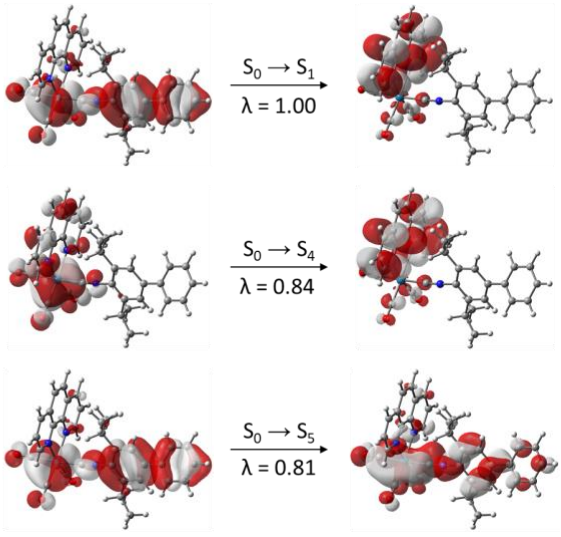


**Figure S11**. (Left) Energies and composition of the lowest energy singlet transitions in **2**. (Right) The natural transition orbitals of transitions $S_0 \rightarrow S_1$, $S_0 \rightarrow S_4$, and $S_0 \rightarrow S_5$ in **2**; λ is the fraction of the hole–particle contribution to the excitation. Calculations performed at DFT//M06/Def2-SVP/SDD level of theory.

[Re(phen)(CO)$_3$(PhEthDippCN)](PF$_6$)

| Transitions | Energy/eV (nm) | *f* | Composition | CI |
|---|---|---|---|---|
| $S_0 \rightarrow S_1$ | 3.07 (404) | 0.0075 | H-1 → L<br>H → L | 0.27248<br>0.65004 |
| $S_0 \rightarrow S_2$ | 3.34 (372) | 0.5193 | H-1 → L+1<br>H → L+1<br>H → L+2 | 0.17169<br>0.54761<br>0.39658 |
| $S_0 \rightarrow S_3$ | 3.35 (370) | 0.8285 | H-2 → L<br>H-1 → L+1<br>H → L+1<br>H → L+2 | 0.21844<br>0.12465<br>0.37896<br>0.52143 |
| $S_0 \rightarrow S_5$ | 3.56 (348) | 0.1343 | H-3 → L<br>H-2 → L<br>H-1 → L<br>H → L<br>H → L+2 | 0.36879<br>0.48884<br>0.24784<br>0.12149<br>0.14131 |

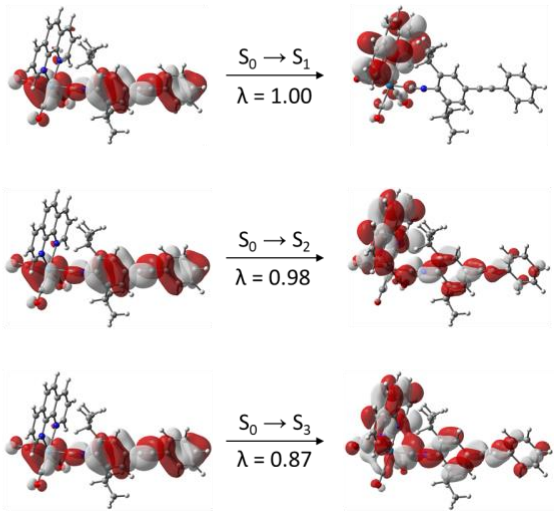


**Figure S12**. (Left) Energies and composition of the lowest energy singlet transitions in **3**. (Right) The natural transition orbitals of transitions $S_0 \rightarrow S_1$, $S_0 \rightarrow S_2$, and $S_0 \rightarrow S_3$ in **3**; λ is the fraction of the hole–particle contribution to the excitation. Calculations performed at DFT//M06/Def2-SVP/SDD level of theory.

[Re(phen)(CO)$_3$(DiPhDippCN)](PF$_6$)

| Transitions | Energy/eV (nm) | *f* | Composition | CI |
|---|---|---|---|---|
| $S_0 \rightarrow S_1$ | 3.06 (406) | 0.0041 | H-1 → L<br>H → L | 0.31148<br>0.63048 |
| $S_0 \rightarrow S_3$ | 3.42 (363) | 0.7760 | H-4 → L<br>H-2 → L<br>H-1 → L+2<br>H → L+2 | 0.12531<br>0.41895<br>0.16694<br>0.51112 |
| $S_0 \rightarrow S_4$ | 3.49 (355) | 0.0113 | H-7 → L<br>H-4 → L<br>H-1 → L<br>H → L | 0.18680<br>0.29838<br>0.53392<br>0.28465 |
| $S_0 \rightarrow S_5$ | 3.50 (354) | 0.2881 | H-4 → L<br>H-2 → L<br>H-1 → L<br>H → L<br>H → L+2 | 0.50187<br>0.25091<br>0.21812<br>0.12807<br>0.31017 |

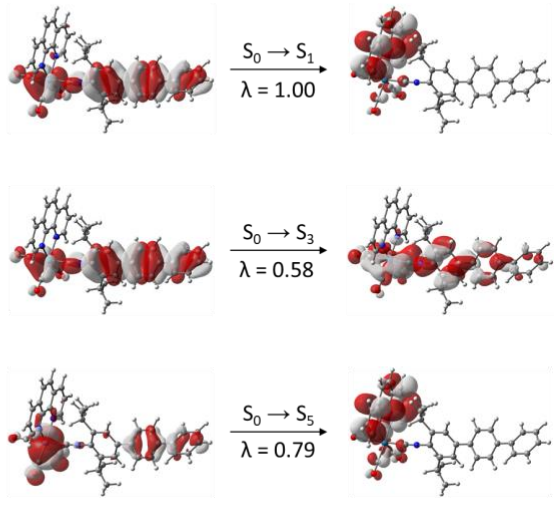


**Figure S13**. (Left) Energies and composition of the lowest energy singlet transitions in **4**. (Right) The natural transition orbitals of transitions $S_0 \rightarrow S_1$, $S_0 \rightarrow S_3$, and $S_0 \rightarrow S_5$ in **4**; λ is the fraction of the hole–particle contribution to the excitation. Calculations performed at DFT//M06/Def2-SVP/SDD level of theory.

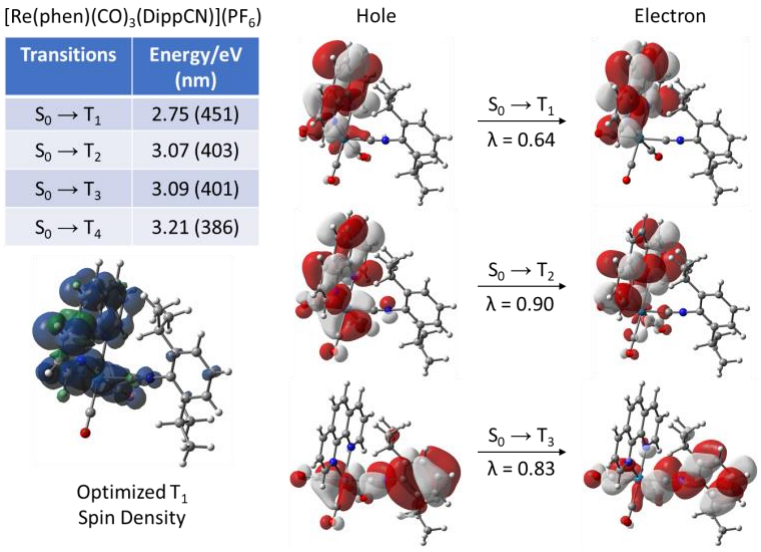


**Figure S14**. (Top-left) Energies of the lowest energy triplet transitions in **1**. (Bottom-left) Optimized $T_1$ state spin density of **1**. (Right) The natural transition orbitals of transitions $S_0 \rightarrow T_1$, $S_0 \rightarrow T_2$, and $S_0 \rightarrow T_3$ in **1**; λ is the fraction of the hole–particle contribution to the excitation. Calculations performed at DFT//M06/Def2-SVP/SDD level of theory.

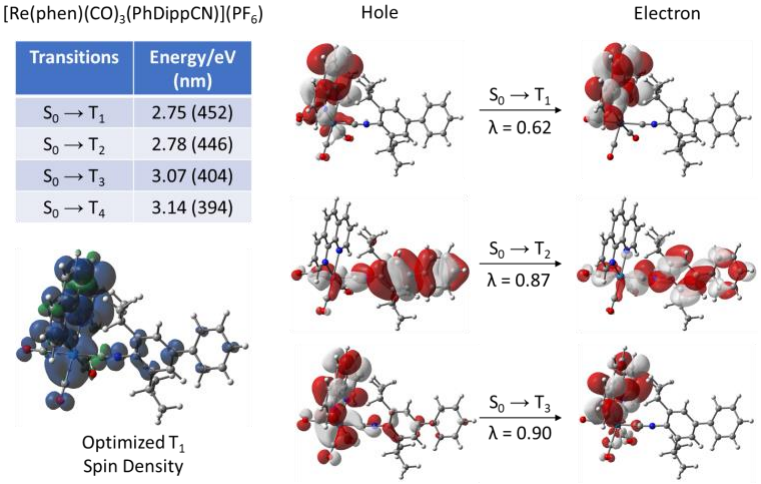


**Figure S15**. (Top-left) Energies of the lowest energy triplet transitions in **2**. (Bottom-left) Optimized $T_1$ state spin density of **2**. (Right) The natural transition orbitals of transitions $S_0 \rightarrow T_1$, $S_0 \rightarrow T_2$, and $S_0 \rightarrow T_3$ in **2**; λ is the fraction of the hole–particle contribution to the excitation. Calculations performed at DFT//M06/Def2-SVP/SDD level of theory.

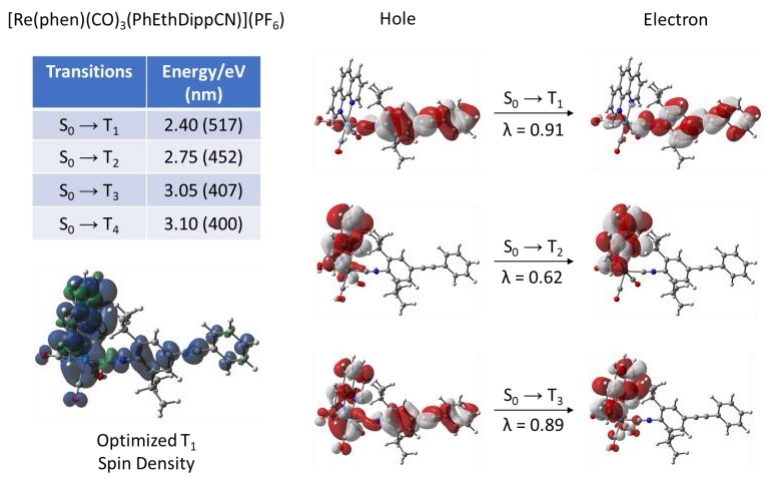


**Figure S16**. (Top-left) Energies of the lowest energy triplet transitions in **3**. (Bottom-left) Optimized $T_1$ state spin density of **3**. (Right) The natural transition orbitals of transitions $S_0 \rightarrow T_1$, $S_0 \rightarrow T_2$, and $S_0 \rightarrow T_3$ in **3**; λ is the fraction of the hole–particle contribution to the excitation. Calculations performed at DFT//M06/Def2-SVP/SDD level of theory.

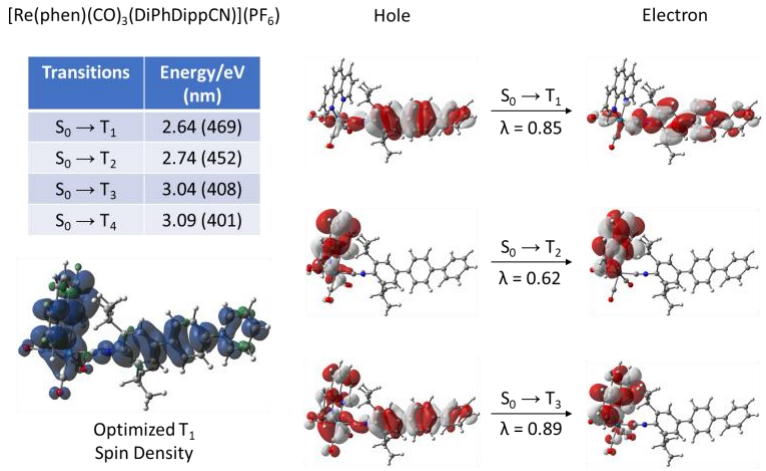


**Figure S17**. (Top-left) Energies of the lowest energy triplet transitions in **4**. (Bottom-left) Optimized $T_1$ state spin density of **4**. (Right) The natural transition orbitals of transitions $S_0 \rightarrow T_1$, $S_0 \rightarrow T_2$, and $S_0 \rightarrow T_3$ in **4**; λ is the fraction of the hole–particle contribution to the excitation. Calculations performed at DFT//M06/Def2-SVP/SDD level of theory.

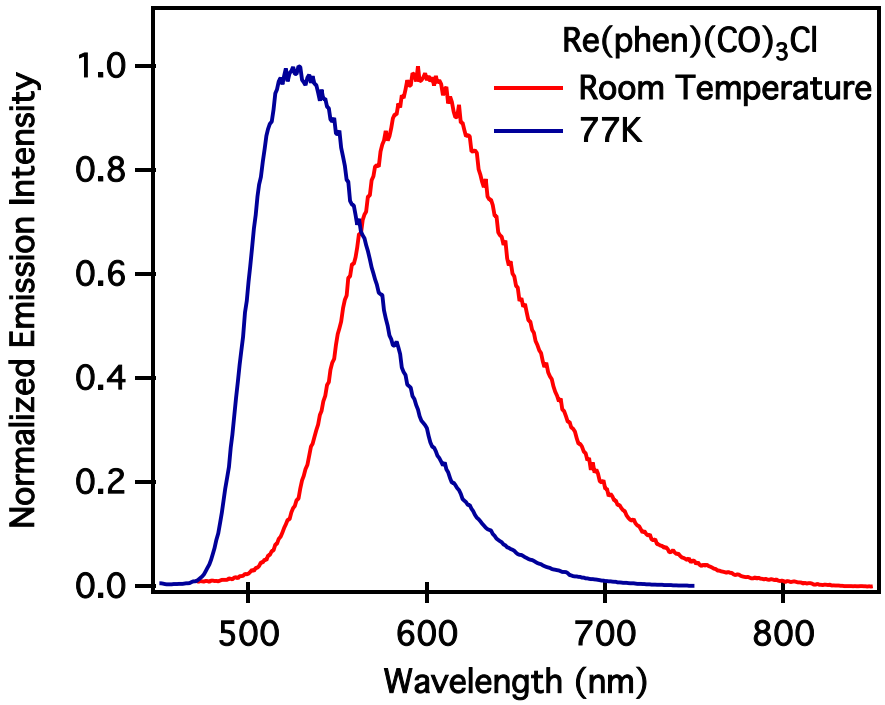


**Figure S18:** Low temperature (blue) and room temperature (red) emission spectra of Re(phen)$(CO)_3$Cl. Spectra recorded 400 nm excitation in THF for R.T. and in 2-MeTHF frozen glass at 77K.

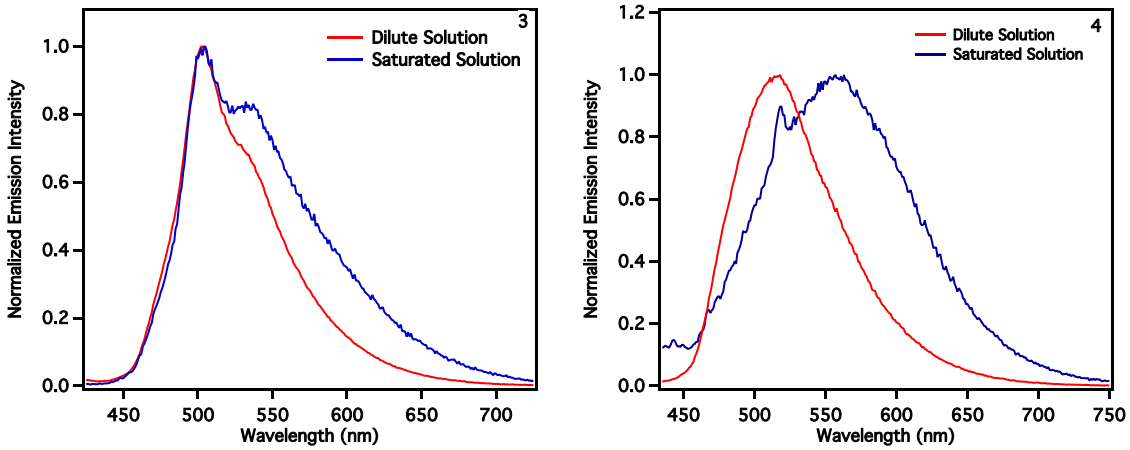


**Figure S19:** Static PL spectra of **3** (left) and **4** (right) showing excimer emission in saturated solution. Excitation at 355 nm. Dilute solutions OD = ~0.1 at excitation.

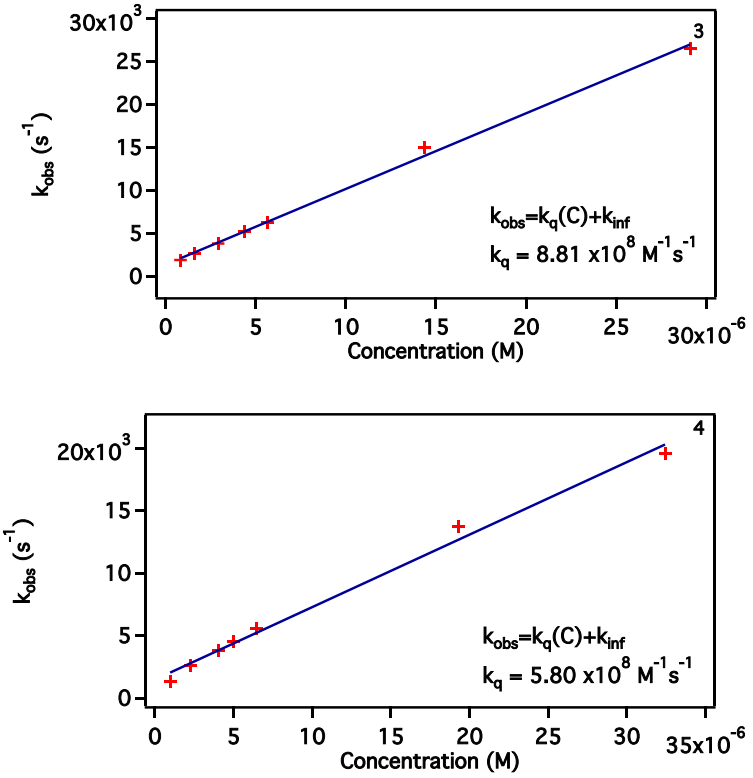


**Figure S20:** Stern-Volmer self-quenching plots of **3** (top) and **4** (bottom).

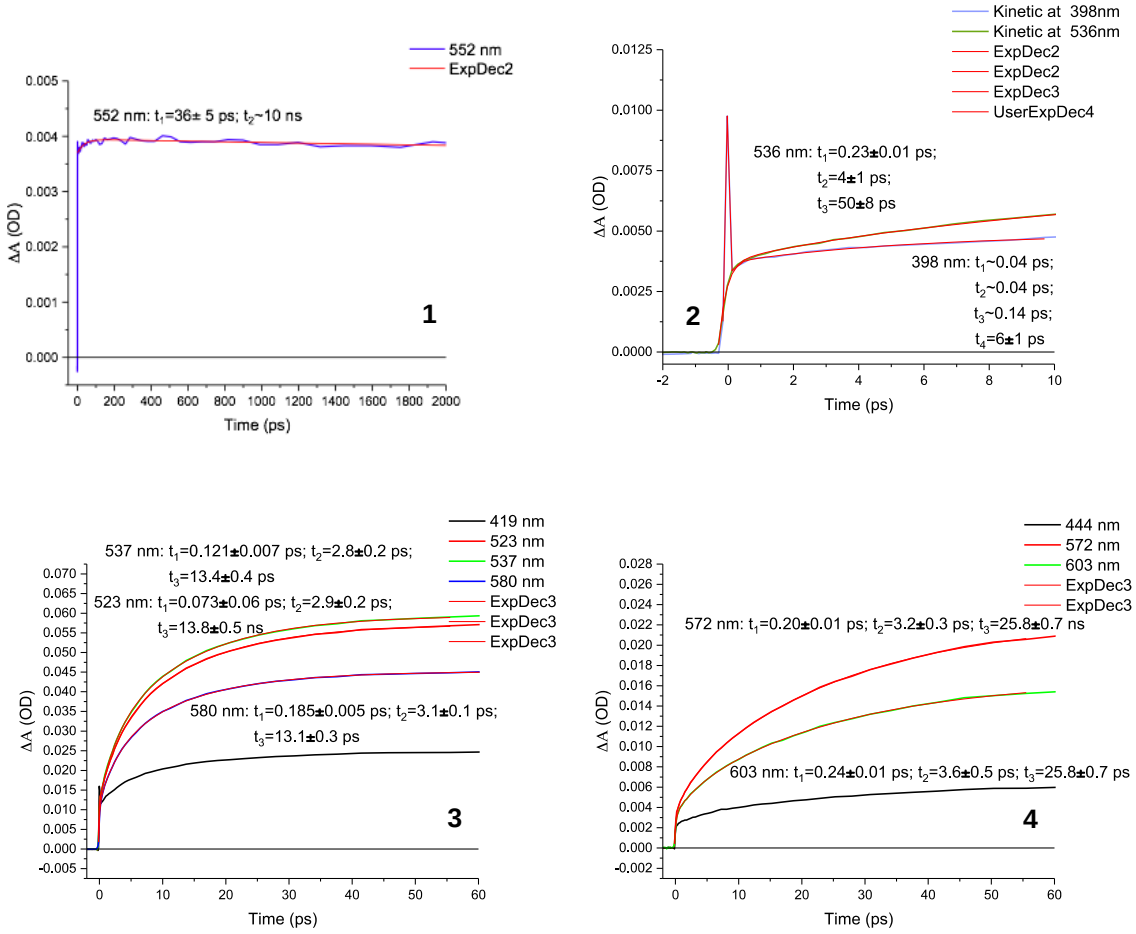


**Figure S21:** Ultrafast TA kinetics of **1**-**4** with best fits.

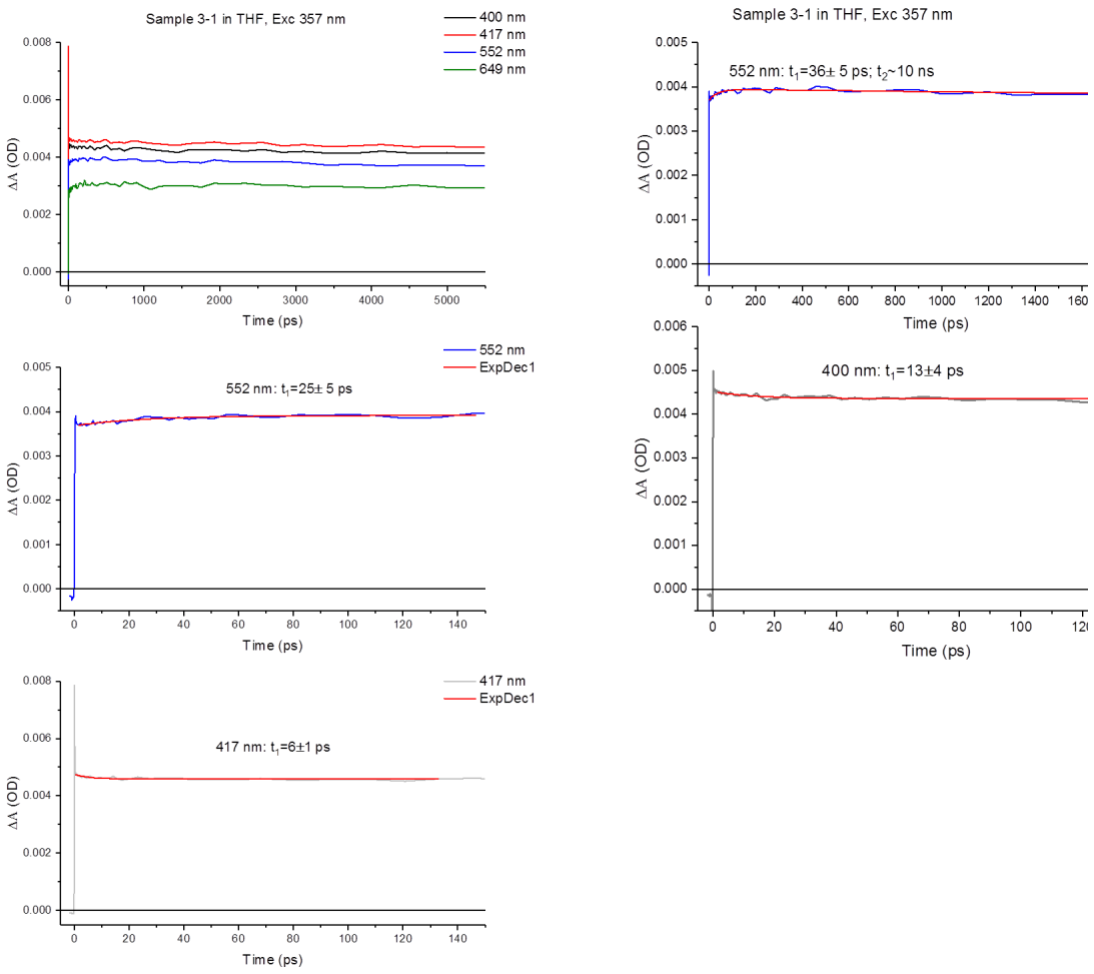


**Figure S22:** Ultrafast TA kinetics of **1** with best fits at various wavelengths.

Visual inspection of kinetic traces at 400, 417, 552, and 649 nm reveal that on a scale of a few tens of picoseconds, the decays in 400 and 417 nm traces look concomitant with the rises at 552 and 649 nm. Low range of change in ΔOD at 400 and 417 nm and remnants of coherent solvent response at 417 nm result in a poor goodness of fit; fitting with a single exponential function result in 13±4 and 6±1 ps time constants, respectively. Fits at 552 and 649 nm result in 25±5 or 36±5 ps time constants with a little better goodness of fit. We assess that this kinetic component is somewhere between 15 and 35-36 ps.

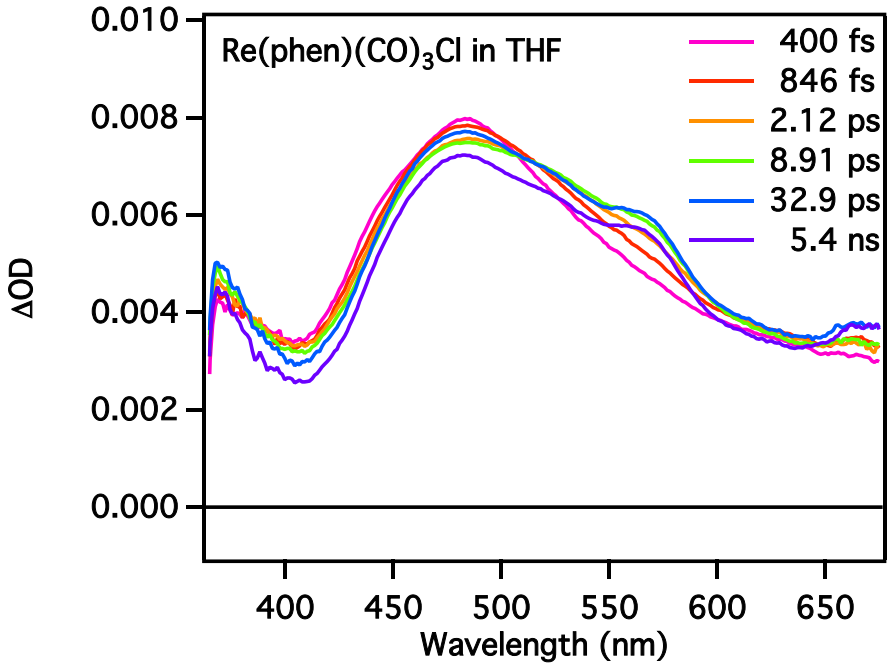


**Figure S23:** Ultrafast TA difference spectra of Re(phen)$(CO)_3$Cl in THF. Spectra recorded at each of labeled delay times with 352 nm excitation.

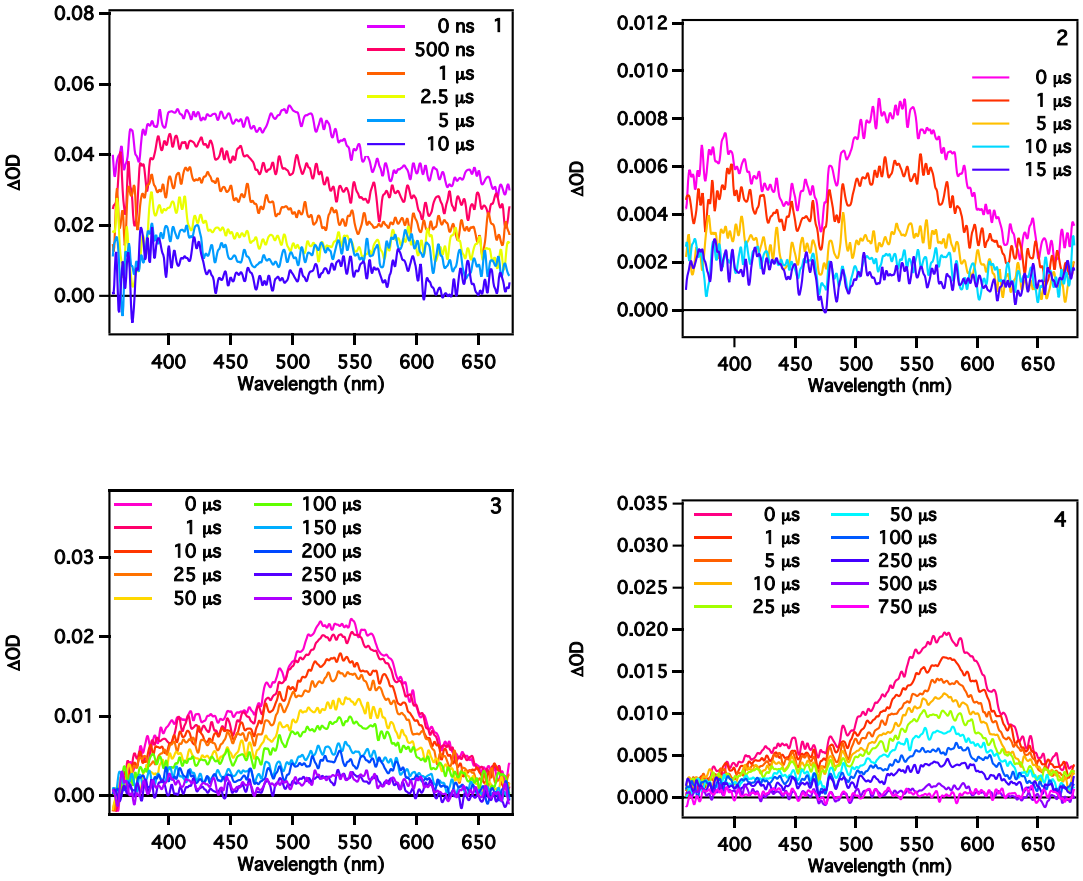


**Figure S24:** ns-TA difference spectra of **1**-**4**. Spectra recorded 355 nm excitation for both.

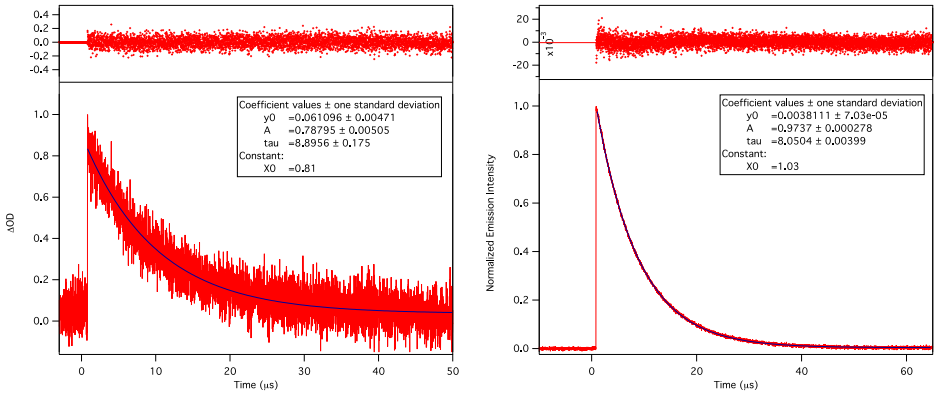


**Figure S25:** ns-TA (left) and PL (right) kinetic decays of **1** with single-exponential fits (blue). ns-TA kinetics recording of 500 nm transient signal with 355 nm excitation. PL kinetics recording of 500 nm emission with 355 nm excitation.

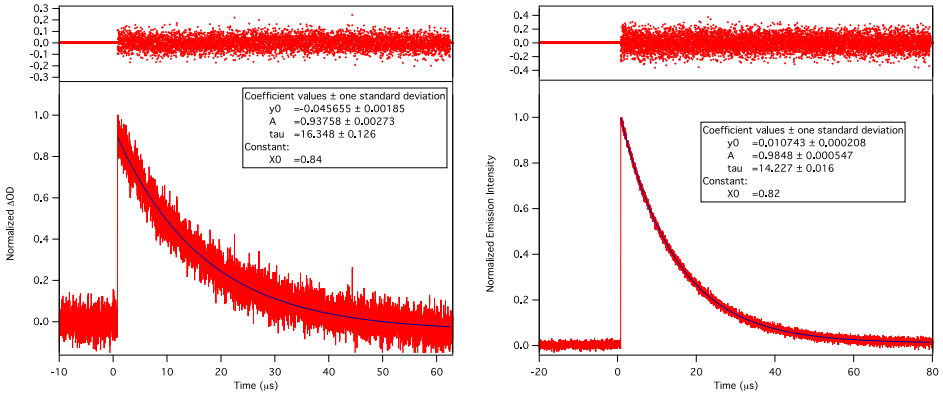


**Figure S26:** ns-TA (left) and PL (right) kinetic decays of **2** with single-exponential fits (blue). ns-TA kinetics recording of 500 nm transient signal with 355 nm excitation. PL kinetics recording of 500 nm emission with 355 nm excitation.

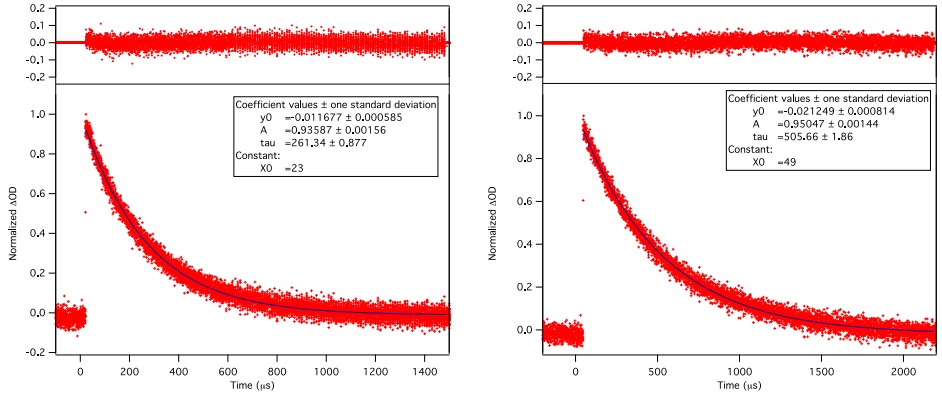


**Figure S27:** ns-TA kinetic decays of **3** (left) and **4** (right) demonstrating single-exponential fits (blue). ns-TA kinetics recording of 550 nm transient signal with 355 nm excitation for both. Sample of **3** OD =˜0.1. Sample of **4** OD =˜0.05

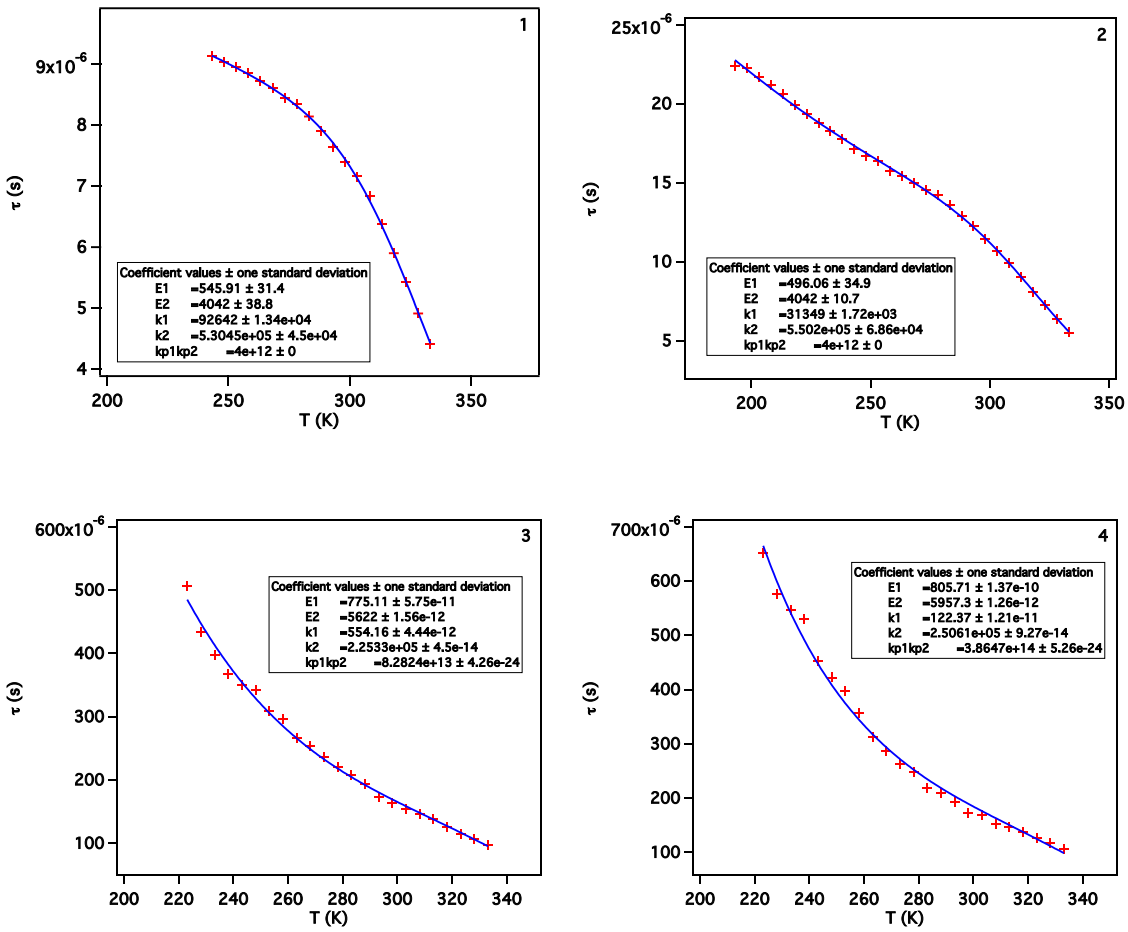


**Figure S28:** Temperature dependent excited state lifetimes with 3-state Boltzmann fits (blue) of **1**-**4**.

References

1. Chow, A. L. F.; So, M. H.; Lu, W.; Zhu, N.; Che, C. M., Synthesis, Photophysical, Properties, and Molecular Aggregation of Gold(I) Complexes Containing Carbon-Donor Ligands. *Chem. Asian J.* **2011,** *6*, 544-553.
2. Sattler, W.; Henling, L. M.; Winkler, J. R.; Gray, H. B., Bespoke Photoreductants: Tungsten Arylisocyanides. *J. Am. Chem. Soc.* **2015,** *137*, 1198-1205.
3. Wrighton, M.; Morse, D. L., Nature of the lowest excited state in tricarbonylchloro-1,10-phenanthrolinerhenium(I) and related complexes. *J. Am. Chem. Soc.* **1974,** *96*, 998-1003.